Modeling of Anti-Cancer Drug Release Kinetics From Liposomes and Micelles: A Review

Nour Al Sawaftah, Vinod Paul, Nahid Awad, and Ghaleb A. Husseini

***Abstract*— Nanocarriers, such as liposomes and micelles, were developed to enhance the delivery of therapeutic drugs to malignant tissues. Internal or external stimuli can be applied to achieve spatiotemporal controlled release from these carriers. This will result in enhancing their therapeutic efficacy while reducing toxicity. Mathematical modeling is used to simulate drug release from nanocarriers; this will facilitate and optimize the development and design of desirable nanocarriers in a systematic manner, rather than a trial-and-error approach. This review summarizes nine mathematical models often used to simulate drug release from nanocarriers and reviews studies which employed these models to simulate drug release from conventional as well as temperature-, pH-, and ultrasound-triggered micelles and liposomes.**

***Index Terms*— Micelles, liposomes, drug release kinetics, mathematical modeling, drug delivery systems.**

I. Introduction

PHARMACEUTICAL nanotechnology has gained considerable attention in the past few decades as promising diagnostic and therapeutic tools, particularly in the field of oncology [1]. Nanocarrier systems offer several advantages such as small sizes compatible with intravenous injection, large surface area per unit volume which enables the alteration of the basic properties and bioavailability of the encapsulated drugs, improved pharmacokinetics, and biodistribution, decreased toxicities, improved solubility and stability, increased circulation time, site-specific delivery of therapeutic agents through surface functionalization, improved patient compliance by reducing the dose and administration frequency and reduced systemic side effects [2], [3]. For this purpose, various nanocarriers possessing unique compositions, morphologies, and surface properties have been developed including, dendrimers, micelles, carbon nanotubes (CNTs), quantum dots (QDs), gold nanoparticles (Au NPs), metal organic frameworks (MOFs), solid lipid nanoparticles (SLNs) and liposomes [4].

Drug release is a determining factor of the absorption/uptake of the therapeutic agent and contributes to the rate and extent of the bioavailability in the body. The aim of spatiotemporally controlled drug release using nanocarriers is to maintain the concentration of the therapeutic agent in the blood or at target tissues at the desired level as long as possible [5]. For spatially controlled drug delivery, nanocarriers are designed to accumulate in tumors through the enhanced permeability and retention (EPR) effect. This effect is caused by the rapid rate of tumor growth and angiogenesis to meet the nutrition and oxygen demands of tumors. Tumor vasculature has an abnormal form and architecture, as it consists of poorly aligned endothelial cells with wide fenestrations and poor lymphatic drainage, where the endothelial pore size varies from 10 to 1000 nm. The passive targeting of nanoparticles (NPs) exploits the EPR effect, and for efficient extravasation from the gaps in the endothelial tissue, NPs should be in the size range of 12.5 nm to 200 nm [6], [7]. Furthermore, receptors overexpressed on tumor cell surfaces have been targeted with nanocarrier platforms decorated with targeting ligands [3]. Actively targeted nanocarriers will recognize and bind to these receptors and are then internalized through receptor-mediated endocytosis [8]–[10].

Stimuli-responsive nanocarriers present an emerging platform to deliver and release payloads in a controlled manner. The unique features of the tumor microenvironment, such as the temperature and pH difference between the tumor and the surrounding tissues, as well as enzyme activation and redox potential, can serve as endogenous triggers for drug release. Drug release can also be triggered using external stimuli such as light, ultrasound (US), magnetic as well as electric fields [11]. Tissue penetration, selective energy deposition, and cost are important considerations when selecting a suitable stimulus. Magnetic fields, light and microwaves have low penetration ability and are therefore limited to surface tumors. Magnetic fields are also costly, and x-rays involve ionizing radiation. US, on the other hand, consists of mechanical waves with frequencies above the audible range (>20 kHz). It can be used to achieve spatiotemporal control of drug delivery and thus, provides a promising approach to treat certain types of cancer. The biological effects of US can be classified into thermal or mechanical effects. The thermal effect of US (US-induced hyperthermia) is represented by a temperature

Manuscript received October 6, 2020; revised February 14, 2021 and May 17, 2021; accepted July 12, 2021. Date of publication July 16, 2021; date of current version October 1, 2021. This work was supported in part by the American University of Sharjah Faculty Research Grants under Grant FRG20-L-48 and Grant eFRG18-BBR-CEN-03, in part by the Al-Jalila Foundation under Grant AJF 2015555, in part by the Al Qasimi Foundation, in part by the Patient's Friends Committee-Sharjah, in part by the Biosciences and Bioengineering Research Institute under Grant BBRI18-CEN-11, in part by the GCC Co-Fund Program under Grant IRF17-003, in part by the Takamul Program under Grant POC-00028-18, in part by the Technology Innovation Pioneer (TIP) Healthcare Awards, and in part by the Dana Gas Endowed Chair for Chemical Engineering. *(Corresponding author: Ghaleb A. Husseini.)*

The authors are with the Chemical Engineering Department, American University of Sharjah, Sharjah, United Arab Emirates (e-mail: ghusseini@aus.edu).

This article has supplementary downloadable material available at https://doi.org/10.1109/TNB.2021.3097909, provided by the authors.

Digital Object Identifier 10.1109/TNB.2021.3097909

TABLE I
COMPARISON BETWEEN DIFFERENT PHYSICAL STIMULI FOR LOCAL DRUG DELIVERY [21]–[24].

Stimulus	Penetration depth	Radiation exposure	Advantages	Disadvantages
Visible/near infrared Light	1-10 cm	No	Very precise, inexpensive, minimally invasive and provides functional information	Limited tissue penetration
X-rays	No limit	Yes	Very precise	Ionizing radiation and high cost
Magnetic field	No limit	No	Energy modulation with an AMF, Provides imaging opportunity	Expensive, limited to surface tumors, accumulation of particles within a magnetic field can lead to embolism and/or increased cytotoxicity
Ultrasound	Several cm	No	Non-invasive, low cost, fast, easily accessible, spatiotemporal control, high patient acceptability and synergism with therapeutic agents	Difficult to apply homogeneously to large volumes and can lead to temperature rise
Microwave	-	No	Non-invasive, easy to generate and control and homogeneous	Low penetration and can lead to temperature rise

rise in the target tissues due to the absorption of energy produced by US waves. On the other hand, the mechanical effects manifest in the form of acoustic cavitation, which includes the formation, growth, and collapse of gas-filled cavities in a medium due to pressure changes. US-responsive nanocarriers are stable while circulating through the body but destabilize when exposed to the thermal effects of US, mechanical effects of US, or a combination of both [12]. US-mediated drug delivery is non-invasive and readily available with high penetration ability. TABLE I compares the different triggering mechanisms used with nanocarriers.

Drug release refers to how drug solutes migrate from the initial position in a drug delivery system to its outer surface and then to the release medium. This seemingly simple process is affected by multiple complex factors such as the physicochemical properties of the solute/drug, the structural characteristics of the system, the release environment, and any possible interactions between these factors [13]. There are many mechanisms that contribute to drug release; some of the main mechanisms are dissolution, partitioning, diffusion, osmosis, swelling, and erosion [14]. To sustain the drug concentration within the therapeutic window at the site of action over a period of time, the drug has to be released in a controlled manner. Mathematical modeling, which describes the relationship of drug release as a function of time, has been very useful in predicting drug release kinetics, and measuring various physical parameters [5]. Introducing mathematical modeling into the drug development process is essential to developing a better understanding of how the drug is released and the factors affecting this process and can be greatly beneficial in designing and optimizing new pharmaceutical formulations.

To the best of our knowledge, this is the first comprehensive review that summarizes the general release characteristics and mechanisms from nanocarriers and the nine model-dependent mathematical models that best fit these release profiles (zero order, first order, Higuchi, Korsemeyer-Peppas, Hixson-Crowell, Baker-Lonsdale, Gompertz, Weibull, and Hopfenberg model). In addition to the mathematical formula, TABLE II provides the assumptions and applications of each model.

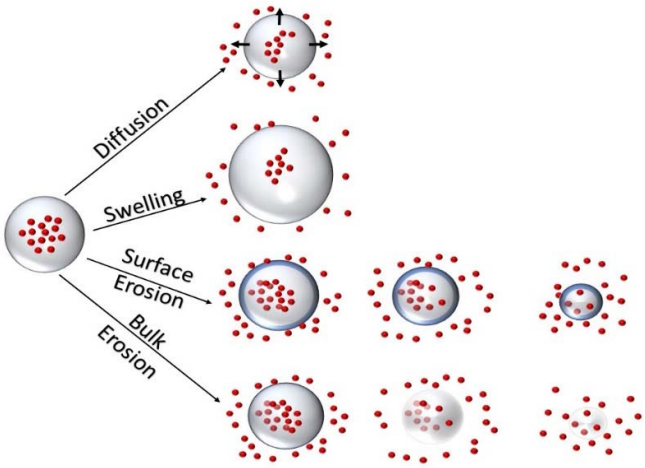

Fig. 1. Drug release mechanisms from nanocarriers.

Furthermore, we reviewed different studies that utilize kinetic models to represent the three most prevalent drug delivery triggering mechanisms (temperature, pH and US).

II. DRUG RELEASE MECHANISMS

One of the main objectives of controlled drug release systems is to maintain the drug level in blood or target tissues within the therapeutic window, i.e., between the minimum effective concentration (MEC) and the minimum toxic concentration (MTC), refer to Figure 1. Drug release from nanocarriers is affected by several factors, including the composition and ratio of drugs, polymers and additives, the physical and chemical interactions among the components, as well as the preparation method. Accordingly, drug release mechanisms can be classified into four categories, diffusion, solvent-, chemical reaction-, and stimuli-controlled release [1], [5], [15].

A. Diffusion-Controlled Drug Release

Diffusion-controlled drug release is driven by a concentration gradient across the membrane, where the drug first dissolves in the core, then diffuses through the membrane [1], [15]. Diffusional mass transport is represented mathematically by Fick's law of diffusion. Adolf Eugen Fick

first described this very important phenomenon in a quantitative way in his article, published in 1855 and titled "About Diffusion" in Poggendorff's Annalen der Physik [13]. The governing principle is that a solute diffuses from regions of higher concentration to regions of lower concentration. Considering all three spatial cartesian dimensions, x, y, and z, and allowing the diffusion coefficient to vary with position, time, and/or solute concentration, the generalized Fick's law of diffusion equation is [14]:

$$\frac{\partial c}{\partial t} = \frac{\partial}{\partial x}\left(D\frac{\partial c}{\partial x}\right) + \frac{\partial}{\partial y}\left(D\frac{\partial c}{\partial y}\right) + \frac{\partial}{\partial z}\left(D\frac{\partial c}{\partial z}\right) \quad (1)$$

where c represents the concentration, t is time, and D is the diffusion coefficient. This expression can be simplified if the diffusivity is independent of time, space, and concentration, and the diffusion equation can be solved when the initial and boundary conditions are specified.

The rate of diffusion depends on the partition and diffusion coefficients of the drug in the membrane, the system geometry (available surface area and membrane thickness), and the drug concentration gradient, whereas the release kinetics depend on the shape of the nanovehicles [16]. If the drug and the release rate controlling material are shaped according to a core-shell structure, with the drug located in the center and the release rate controlling material forming a membrane surrounding this core, then the system is referred to as a "reservoir system." However, if the drug is homogeneously distributed in a continuous matrix formed by the release rate controlling material, then the system is referred to as a "monolithic system" [14], [17].

An extensive collection of analytical solutions of Fick's law of diffusion for different geometries as well as initial and boundary conditions is provided by Crank [18]. However, no analytical solution of Fick's law is available for delivery systems with time-, position-, or concentration-dependent diffusion coefficients, and systems with complex shapes. In such cases, numerical techniques are used to determine mass transport [14].

B. Solvent-Controlled Drug Release

Solvent-controlled drug release is further divided into osmosis- and swelling-controlled release. Osmosis-controlled release takes place when semi-permeable polymer membranes are uniformly loaded with highly soluble drugs. Water can flow from the region of low drug concentration (outside the carrier) to the region with high drug concentration (drug-loaded core). As a result, the local osmotic pressure becomes very high and causes the carrier to rupture and release its contents [1], [15]. The Kedem–Katchalsky (K–K) equations and their improved versions [17] are usually used to describe the volume flow of water or water flux into the core [19], [20].

$$\frac{dv}{dt} = \frac{A}{h}L_p(\sigma d\pi - dp) \quad (2)$$

where dv/dt is water flux, A is area of the semi-permeable membrane, h is the thickness of the membrane, $d\pi$ and dp are the osmotic and hydrostatic pressure difference between the inside and outside of the system respectively, L_p is mechanical permeability and σ is the reflection coefficient. This mechanism usually results in a zero-order release profile as long as a constant concentration gradient is maintained across the membrane [1], [15].

Swelling-controlled drug delivery systems refer to systems in which the swelling of the carrier is the release rate-controlling step. This phenomenon can be accompanied by other mass transport processes, such as drug dissolution, drug diffusion, and polymer dissolution [14]. Swelling-controlled drug delivery systems are often based on hydrophilic glassy polymers, such as hydroxypropyl methylcellulose. Upon contact with water or buffer, the polymer chains relax, leading to the swelling of the system. In order to induce polymer chain relaxation, a minimum water concentration is required. This limit is a function of the physicochemical characteristics of the polymer (i.e., the chemical structure of the backbone and side chains, average polymer molecular weight), and temperature. Once the minimum water requirement is met, two processes/phenomena occur in sequence: (1) water diffusion and (2) polymer chain relaxation. If one of these processes is much slower than the other, the slowest step controls the drug release kinetics from the system [1], [14], [15], [25]. Drug release from swellable systems can be quantified using the semi-empirical Korsmeyer-Peppas model [14], [25]:

$$\frac{M_t}{M_\infty} = kt^n \quad (3)$$

where M_t and M_∞ denote the absolute cumulative amounts of drug released at time t and infinity, respectively; k is the rate constant, and n is the release exponent. The constant rate k, and release exponent n depend on the dosage form geometry, the dominating process (i.e., relaxation or diffusion), and structural factors governing diffusion and relaxation rates. If the polymer relaxation process is the slowest step, then zero-order drug release kinetics result and the above equation becomes [14]:

$$\frac{M_t}{M_\infty} = kt \quad (4)$$

However, if the dosage form is thick or has a spherical or cylindrical geometry, then the surface area of the swelling front generally decreases with time, which means that the release rate decreases with time, and the release exponent would have a value other than unity. Similar equations can be obtained when diffusion is the dominant process. However, no other phenomena (e.g., limited drug solubility or inhomogeneous initial drug distribution) are important, as they may lead to similar n values as pure swelling or pure diffusion control. When n values are observed between 0.5 and 1 for slabs, 0.45 and 0.89 for cylinders, and 0.43 and 0.85 for spheres, diffusional mass transport, and polymer chain relaxation may both be rate-controlling processes. In such cases, the drug release mechanism is referred to as "anomalous transport" [1], [14], [15].

For hydrophilic polymer chains, erosion might also play a significant role in controlling the rate of drug release. Upon contact with aqueous media, water content significantly increases, resulting in increased chain mobility. As a result, the chains start to disentangle at certain positions and re-entangle at others. If the water content is higher than the

polymer content, then the number of disentanglements will exceed the number of new entanglements, and the network erodes into the bulk fluid. If the incorporated drug is initially present in the form of solid particles, upon contact with water, these particles start to dissolve [14]. The dissolution of the drug is governed by three theories: the diffusion layer model (film theory), Danckwert's model (surface renewal theory), and double barrier theory [26].

The diffusion layer model involves two steps, the dissolution of the solid to form a stagnant film which is saturated with the drug, followed by the diffusion of the solubilized drug from the stagnant film into the bulk of the solution (this being the rate-determining step of the process) [27]. The diffusion layer model can be represented mathematically by the following equations [28]–[31]:

1. Noyes-Whitney equation: this equation is used to describe the process of solid dissolution and is based on Fick's second law of diffusion. The following assumptions are made when using this equation: (1) the system is spherical in shape, (2) the drug dissolves uniformly from all surfaces, (3) the thickness of the diffusion boundary is constant, and (4) the thickness of the diffusion boundary is independent of the particle size. Accordingly, the mathematical representation of the Noyes-Whitney rule is as follows [14]:
$$\frac{dm}{dt} = kS(C_s - C_t) \tag{5}$$
Here, m represents the mass transferred through dissolution per unit time t, from a solid particle of instantaneous surface S, and k is a constant. The concentration gradient constitutes the driving force for this dissolution process and is represented in the above equation by (C_s-C_t), where C_t is the concentration at time t, and C_s is the equilibrium solubility of the solute. The rate of dissolution dm/dt is the amount dissolved per unit area per unit time. The C_t term can be neglected if it is less than 15% of the saturated solubility C_s. In such a case, the dissolution is said to be occurring under sink conditions. Moreover, the surface area, S is considered constant initially or when the quantity of material present exceeds the saturation solubility.
2. Nernst-Brunner equation: this equation is a modification of the Noyes-Whitney equation in which Fick's first law of diffusion was used to establish a relationship between the constant k and the diffusion coefficient of the solute producing the following equation [28]:
$$k = \frac{DS}{h\gamma} \tag{6}$$

where D is the diffusion coefficient, S is the area of the diffusion layer, γ is the solution volume, and h is the diffusion layer thickness. In formulating this equation, Nernst and Brunner assumed that the process at the surface proceeds much faster than the transport process.

Danckwert's model adds to the diffusion layer model by taking into account the eddies present in an agitated fluid. These eddies or packets take up the solute at the solid-liquid interface and carry it into the bulk of the solution. Another addition was proposed by the double barrier theory. This theory proposes that an intermediate concentration exists at the solid-liquid interface that is a function of solubility rather than diffusion [27], [31], [32].

C. Chemical Controlled Drug Release

Chemically controlled systems can be classified into erodible/degradable and pendant chain systems. The drug release rate in erodible systems is controlled by polymer degradation, while in pendant chain systems, the drug release is controlled by the enzymatic degradation of a chemical bond between the drug and the polymer carrier [15]. Zero-order release can be obtained with pendant chain systems, provided that the cleavage of the drug is the rate-controlling mechanism [33].

There are two mechanisms of erosion: surface and bulk erosion. Bulk erosion refers to the simultaneous degradation of the entire matrix, which is the case with matrices made of polymers like poly(lactic-co-glycolic acid) (PLGA), polylactic acid (PLA), and polycaprolactone (PCL). Whereas, surface erosion refers to the degradation of the system from the surface to the core, which is the case when the carrier system is made up of polyanhydrides and poly(orthoesters) [1], [14], [15]. Surface erosion is ideal for many drug delivery applications because erosion kinetics are controllable and reproducible. Moreover, contrary to bulk erosion, the water permeation rate is slow, ensuring the protection of drugs [33], [34]. However, in nanocarrier systems, where the distance of water diffusion is short, and the domain size of crystallization is restricted, polymer degradation does not necessarily follow the typical surface erosion behavior but tends to show signs of bulk degradation (constant particle size during polymer degradation) [1].

Drug release from surface-eroding polymers can be represented using the Hopfenberg model, where the zero-order surface release of the drug determines the rate-limiting step. The following equation holds true for several geometries (i.e., spheres, cylinders, and slabs).
$$\frac{M_t}{M_\infty} = 1 - \left(1 - \frac{k_0 t}{c_0 a}\right)^n \tag{7}$$

where M_t and M_∞ are the cumulative drug release at time t and infinity, k_0 is the erosion rate constant, c_0 is the initial concentration of the drug, a is the radius of the cylinder/sphere (or half the thickness of the slab), and n is a shape factor (where n = 3 for a sphere, n = 2 for a cylinder, and n = 1 for slabs). A unified model to represent both surface and bulk erosions has been developed. In this model, diffusion-reaction equations are combined with dissolution and pore formation mechanisms to determine drug release [34]. The fraction of drug released, $R(t)$, is expressed as follows [35]:
$$R(t) = 1 - P(t) \tag{8}$$

where $P(t)$ represents the cumulative fraction of the remaining drug in the polymer matrix in time, which can be determined

TABLE II
SUMMARY OF KINETIC MODELS

Model	Equation	Assumptions	Applications
Zero-Order	$\frac{dQ(t)}{dt} = K_0$	Dosage forms do not disintegrate, drug released slowly.	Describes the drug dissolution of several types of modified release dosage forms, some transdermal systems and matrix tablets with low soluble drugs in coated forms, osmotic systems, etc.
First-Order	$\frac{dC(t)}{dt} = -KC(t)$	The change in concentration of the drug is a function of the instantaneous concentration.	For the dissolution of pharmaceutical dosage forms such as those containing water-soluble drugs in porous matrices.
Higuchi	$Q = k_h\sqrt{t}$	The initial drug concentration must be much higher than drug solubility, diffusivity is constant and occurs only in one dimension, the size of drug particles is much smaller than the thickness of the film, carrier material does not swell or dissolve, Perfect sink conditions.	Describes the dissolution of the drug from several types of modified release dosage forms, transdermal systems, and matrix tablets with water soluble drugs.
Korsmeyer-Peppas	$CFR \approx k_{kp}t^n$	The generic equation is applicable for short times, M_t/M_∞<0.6 used to determine n, drug release occurs in one dimension, the system's length-to-thickness ratio is at least 10.	Describes drug release from several modified release dosage forms.
Hixson-Crowell	$\frac{dW}{dT} = \frac{kA(C_s - C_\infty)}{l}$	Dissolution occurs normal to the surface of the solute particles, agitation is uniform over the exposed surface and the particles are spherical.	Applicable to tablets whose dimensions diminish proportionally, and dissolution occurs in planes that are parallel to the drug surface.
Baker-Lonsdale	$\frac{3}{2}\left[1-\left(1-\frac{M_t}{M_\infty}\right)^{\frac{2}{3}}\right]-\frac{M_t}{M_\infty} = \frac{3D_m C_{ms}}{r_0^2 C_0}t$	Variation of the Higuchi model, the matrix is homogenous and has no fractures that will cause unintended release.	Used for linearized release data from several formulations of microcapsules or microspheres.
Gompertz	$X(t) = X_{max}\exp\left[-\alpha e^{\beta\, log(t)}\right]$	Good stability and an intermediate release rate.	To describe *in vitro* dissolution profiles.
Weibull	$\frac{dN}{dt} = -k' fr(t)N$	Empirical equation, fractal geometry.	To compare the release profiles of matrix drug delivery.
Hopfenberg	$\frac{M_t}{M_\infty} = 1-\left[1-\frac{k_0 t}{C_0 a_0}\right]^n$	Semi-empirical model, overall release behaves as a zero-order.	To identify the release mechanism of the optimized oilispheres.

using the following expression [35]:

$$P(t) = V^{-1}\int \frac{c_s + c_A}{c_{s0}}dV \tag{9}$$

D. Stimuli-Controlled Drug Release

Stimuli-mediated drug release from nanocarriers is controlled by internal or external stimuli such as temperature, pH, ionic strength, US, electric or magnetic fields [1], [36]. Stimuli-responsive carriers are designed to remain stable while circulating through the body but once they are exposed to a certain stimulus, they destabilize and release their contents. The release can either obey Fickian diffusion, anomalous transport, or case II transport. An interesting aspect of stimuli-controlled release is that it can be completely reversible. This type of behavior may allow these materials to serve as self-regulated, pulsatile drug delivery systems [1], [33].

III. MATHEMATICAL MODELING OF DRUG RELEASE

Incorporating mathematical models into the design process of drug delivery systems offers numerous advantages, including better estimates of the compositions, dimensions and geometry of the delivery systems, as well as accounting for administration route, drug dose and release profile [14], [28], [31]. All of which are factors that would significantly reduce the amount of experimentation needed during product development, hence saving both time and capital. Moreover, such quantitative analyses of the phenomena involved in drug release permit a better understanding of the mechanisms underlying drug release, which in turn would help improve the safety of the developed products [28], [31], [37].

The quantitative approach towards drug release began with the famous equation developed by Professor Takeru Higuchi to quantify drug release from thin ointment films.

Ever since, various models, varying in accuracy and complexity, have been proposed, including empirical and semi-empirical models, as well as mechanistic-realistic ones [37], [38].

While empirical and semi-empirical models provide a purely descriptive mathematical treatment, mechanistic-realistic models are founded on well-established scientific phenomena such as diffusion, dissolution, swelling and precipitation. Consequently, these models permit the determination

of system-specific parameters and the effects these parameters have on drug release kinetics. In addition, the required composition, size, shape and preparation procedure of a novel treatment become theoretically predictable [28], [31], [37], [39].

When developing and/or using mathematical models to quantify drug release, the following aspects need to be taken into consideration [14], [31], [37]:

I. The accuracy of the model generally increases with increased complexity. That is, the more physical, chemical, or biological phenomena included, the more complex, yet, realistic the model becomes.
II. Theoretical calculations should always be compared to experimental results. This can be achieved either by fitting the theory to experimental data, or theoretical predictions can be compared with independent experimental results.
III. There is no universal mathematical theory that can be applied to all types of drug delivery systems. Some models are applicable to a very limited number of drug delivery systems, whereas others have a broader scope of application.

In addition to the underlying drug release mechanisms, mathematical models must take into account the type of drug(s), incorporated drug dose, preparation technique, environmental conditions during drug release, as well as the geometry and dimensions of the drug delivery system. Presently, most models treat the human body as one or two well-stirred compartments. Biological processes such as enzymatic degradation, intra-cellular drug transport, interactions with compounds in the extra- and intracellular space, drainage into the lymphatic system, transport across the blood-brain-barrier (BBB) and other such complications are not included. In the future, it will be of major importance to account for these events to achieve more holistic and realistic mathematical theories [31], [37], [39].

The methods to investigate the kinetics of drug release from controlled-release dosage formulations can be classified into three categories: (1) statistical methods, (2) model-dependent methods, and (3) model-independent methods [28]. This review focuses on model-dependent models/methods; for a more detailed discussion of the statistical and model-independent methods for modeling drug release, the reader may refer to [31], [40]–[45].

Model-dependent methods use different mathematical functions to describe the release profile. Once a suitable function has been selected, the model parameters are used to evaluate the release profile. Deciding on a suitable function is usually carried out using non-linear regression analyses [31], [46], [47]. Various types of models can be used to simulate drug release kinetics, including zero-order, first-order, Higuchi, Baker-Lonsdale, Hixson-Crowell, Weibull, Gompertz, Hopfenberg and Korsmeyer-Peppas models. TABLE II summarizes these models, the assumptions they are based on and their applications. Detailed derivations of the models are provided in the supplementary material.

IV. Kinetic Modeling of Drug Release From Micelles and Liposomes for Cancer Therapy

Solid tumors are characterized by a disordered microvasculature that favors the accumulation of large biomolecules and nanocarriers [48]. Nanocarriers such as micelles and liposomes have shown great potential in cancer targeting owing to their ability to accumulate in the tumor region via the EPR effect [10], [49]–[51]. Micelles are biocompatible, core–shell structures made up of amphiphilic molecules such as lipids or polymers. When exposed to an aqueous environment, the component molecules of the micellar systems arrange themselves into monolayer spherical vesicles with the hydrophobic cores hidden inside the structure, while the hydrophilic groups are directed outwards. Drugs with poor water solubility are loaded inside the micelle's hydrophobic core, whereas hydrophilic drugs tend to align themselves near the hydrophilic components of the micellar structure. Liposomes, on the other hand, are concentric spheres of phospholipid bilayers separated by aqueous compartments. Liposomes are structured in such a way that the outer surface is comprised of the hydrophilic head groups, whereas the hydrophobic tails form the inner part of the structure (refer Figure 2).

Both micelles and liposomes have proven to be effective smart drug delivery systems (SDDSs) due to their ease of preparation, biocompatibility, non-immunogenicity, efficient and versatile loading capacity, controlled release kinetics, and the possibility and ease of functionalization [12], [52].

Generally, drug release from micelles occurs through diffusion or slow degradation of the polymeric material [53]. If the interaction between the polymer and the drug is strong and the rate of biodegradation is fast, the degradation would govern the rate of drug release. However, this is not the prevailing behavior and the rate of drug release from micelles usually exceeds the rate of polymer degradation. Therefore, diffusion of the drug may be considered the principal mechanism of release from micelles. For hydrophobic drugs located in the micellar core, release can follow two major pathways, i.e., dissociation of the micelle followed by the separation of the drug from the monomers or drug–polymer bond breakage within the micelle followed by the diffusion of the payload [54]. With regard to hydrophilic drugs, their release was found to account for the "burst release" from micelles [55].

Several factors affect drug release from micelles, such as the rate of diffusion of the drug, the stability of the micelles, and the rate of biodegradation of the polymer; these factors are in turn influenced by the compatibility between the drug and the constituent polymeric material, length of the polymer, amount of the loaded drug, and the molecular volume of the drug. With respect to drug properties, an increase in the concentration of the drug present often results in a decrease in the rate of drug release; and an increase in the molecular weight and volume of the drug requires the reorientation of polymeric chains, constricting the movement of the drug molecules through the polymer matrix. As a result, larger or heavier molecular weight drugs tend to have lower diffusion coefficients as

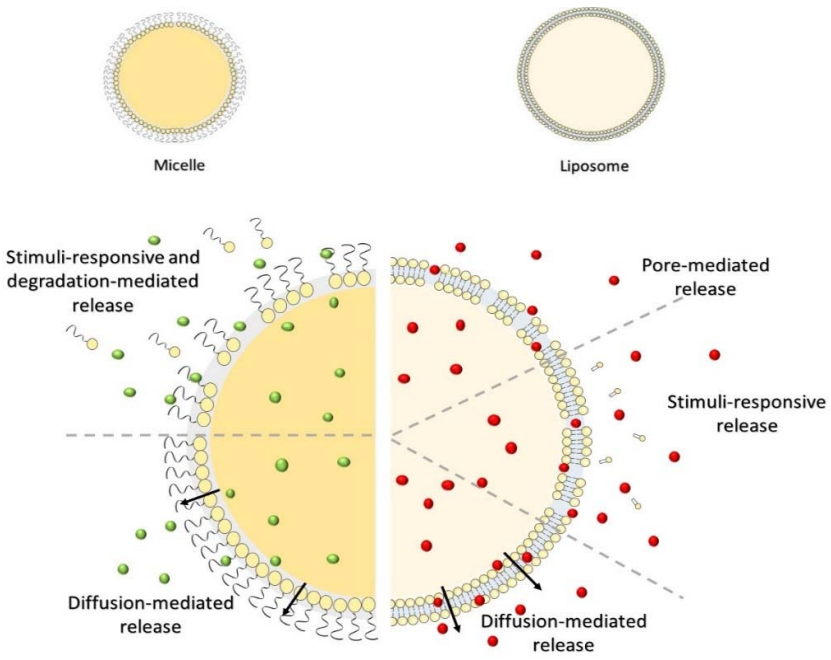

Fig. 2. Plausible release mechanisms from micelles (left), and liposomes (right).

opposed to their smaller molecular weight counterparts. The properties of the micellar core were also found to have a great effect on the rate of diffusion of the drug. Generally, an increase in the molecular weight of the hydrophobic block or the size of the core decreases the overall rate of the release rate of the entrapped agent. Moreover, polymers with a high glass transition temperature or bulky groups on their backbone are limited in terms of their ability to reorient. As a result, the diffusion of molecules from micelles with glassy cores is slower than the diffusion out of cores that are more fluid [39], [55], [56].

Drug release from liposomes occurs as diffusion mediated release (e.g., zero-order and first-order), pore-mediated release, membrane perturbation mediated release or a combination of these mechanisms (e.g., Higuchi) [49]. Drug release from liposomes depends on the properties of both, the encapsulated drug, and the liposomal formulation. Larger liposomes can encapsulate greater amounts of the drug per vesicle compared to smaller ones but tend to have worse biodistribution, slower release and poor injectability. In addition, drug release is highly dependent on the composition of the liposomal formulation. Some of these components can be optimized to achieve the desired release profile, these include amount of cholesterol, number and length of side chains, charge, polar head group, degree of saturation, acyl chain length and the phase transition temperature (T_c).

Generally, liposomes composed of phospholipids in a solid gel phase, with or without a low cholesterol content, retain compounds more efficiently than liposomes composed of phospholipids in a liquid phase. While phospholipids are often the main component of the liposomal membrane, they can be supplemented with other lipids, polymers, and sterols (e.g., cholesterol) to modify and optimize membrane properties such as, stability, rigidity, as well as the release profile. For drug-loaded liposomes, cholesterol is necessary for enhancing the stability of liposomes and maintaining the drug in the liposomal interior. It also plays a prominent role in the maintenance of high plasma levels of liposomes. The length of the acyl chain in lipids may affect drug release through their influence on membrane packing, hydrophobicity, and T_c. Out of these properties, T_c tends to exert the biggest influence on drug release and is in turn affected by the lipid chain length, polar head group and degree of saturation. The T_c of a liposomal formulation can be altered by changing the lipid acyl chain length and by varying the degree of saturation of the constituent lipids. Introducing even one double bond into the lipid chain dramatically reduces lipid T_c [26], [57]–[59].

To establish better *in vitro – in vivo* correlations, the release kinetics models detailed above are continuously used to predict drug release profiles for micelles and liposomes. Fugit *et al.* [60] used mathematical model fitting to predict the drug release kinetics from DOX-loaded liposomes. The model was statistically investigated using the Box-Behnken design for different variables affecting the release rate; the investigated variables included: extravesicular pH, the ammonia concentration in the release medium, and the dilution of the formulation. Dilution of the formulation was not found to affect release kinetics significantly. While low intravesicular pH, in the case of high ammonium concentration, was found to promote acid-catalyzed lipid degradation, which enhanced the release rate of DOX *in vivo*.

Yoon *et al.* [61] investigated the release of Docetaxel (DTX) from RIPL peptide-conjugated liposomes (DTX-RIPL-L). The release studies showed that for both functionalized and peptide-free liposomal formulations, the release followed a biphasic pattern, with a rapid release in an initial period of 6 h, followed by a slower, sustained release up to 72 h. The initial, fast release of drug-loaded liposomes was attributed to DTX adsorbed on the surface of the lipid bilayer; whereas the sustained release thereafter was due to the drug being released

TABLE III
SUMMARY OF RELEVANT STUDIES

Carrier type	Payload	Remarks on drug release	Ref.
Polyelectrolyte-coated liposomes	DOX	• Polyelectrolyte-coated liposomes showed sustained drug release (~35%) following Higuchi kinetics.	[81]
Liposomes	LXT - 101, a cationic amphipathic peptide	• *In vitro* release in NaCl medium at 37°C showed 70–90% LXT-101 release from MVLs over 11 days. • According to the Ritgar-Pepps model, the *in vitro* release of DepoLXT - 101 was governed by Fick's diffusion.	[82]
pH-sensitive bola-type triblock copolymer (PEG m - PDPA n -PEG m) functional hybrid liposomes (liposome@Bola)	DOX	• The Higuchi model predictions were in good agreement with the experimental data. • Drug release from liposomes depended on membrane diffusion, irrespective of the environmental pH.	[83]
Liposomes	-	• The proposed mathematical model acted as the basis for obtaining a more effective drug delivery system and could be modified by including more complexities for any specific tumor-drug interactions.	[84]
Starshaped poly (L-lactide) and tocopheryl polyethylene glycol 1000 succinate copolymeric micelles	Indometacin (IMC)	• The IMC accumulative release can be decreased by increasing the arm numbers of the s-PLLA-TPGS copolymers. • The release profiles of IMC from the s-PLLA-TPGS copolymers followed the Baker-Lonsdale model equation.	[85]
pluronic F-68 micelles	DTX	• The Higuchi and Baker-Lonsdale models were the best fit for the release kinetics. • Drug is released through diffusion without the swelling and dissolution of the delivery system.	[86]
mPEG–PCL copolymeric micelles	Naproxen	• Naproxen release data adequately fit Makoid–Banakar, Weibull, Logistic, and Gompertz models. • Drug release from Naproxen conjugated mPEG–PCL micelles is complicated and could not be illustrated easily by these mathematical representations.	[87]

from the inner layers. The results of the release experiments were fitted to several models, including zero-order, first-order, and Higuchi equations. Overall, the first-order model provided the best fit, but the Higuchi model also showed a relatively good correlation. Focusing on the first-order kinetic analysis, the release rate constant was significantly reduced by liposomal encapsulation (0.2029/h for DTX-Sol versus 0.0341/h for DTX-EL), and further decreased by surface modification with the RIPL peptide (0.0265/h for DTX-RIPL-L). These results indicated that the liposomal bilayer and peptide modification present additional barriers to drug diffusion.

Lu *et al.* [62] investigated the release from DTX-loaded PEGylated triacontanol (mPEG2k-b-TRIA) micelles. The drug release followed first-order kinetics, thus enabling prolonged release. In another study, Lapenda *et al.* [63] studies the *in vitro* kinetic profiles of trans-dehydrocrotonin (t-DCTN) loaded liposomes and its t-DCTN:hydropropyl-_-cyclodextrin (HP-_-CD) loaded liposomes to improve t-DCTN antitumor activity. The kinetics were fitted with and showed great agreement with the Fickian square-root-of-time ($t^{1/2}$) model.

V. KINETIC MODELIING OF TEMPERATURE, PH AND US TRIGGERED DRUG RELEASE FROM MICELLES AND LIPOSOMES

As mentioned earlier, stimuli-responsive nanocarriers are designed to destabilize and release their payload upon exposure to a specific stimulus. In terms of release, stimuli-responsive micelles and liposomes offer the following advantages, better solubilization of hydrophobic drugs, prolongation of the drug circulation time, and release of guest molecules in a controlled manner [53]. Studying the release kinetics of stimuli-responsive micelles and liposomes is a relatively new field; therefore, proper fitting of release kinetics is essential for modeling and optimizing drug release and drug accumulation via these systems [64]. Haghiralsadat *et al.* ([65] investigated the kinetics of doxorubicin (DOX) release from nano-liposomes as a function of temperature and pH. The long-term sustained release behavior of DOX was found to be governed by three mechanisms: (1) the slow rate of solubilization of aggregated DOX inside the liposome, (2) the diffusion of dissolved DOX from the liposome and transfer to outside the dialysis tube and (3) the dispersion of DOX molecules by a convection mechanism due to the gentle shaking of PBS solution. The results showed a slow drug release rate at higher pH values and lower temperatures (43% accumulated release reached at 96 h for 42 °C and pH = 5.4 while just 33% of DOX was released for 37 °C and pH = 7.4). This phenomenon demonstrated that a lower pH (5.4) tends to increase the hydrophilicity of DOX and solubilization inside the liposome, which in turn accelerated drug release. Another explanation for the fast drug release is that at high temperatures (42 °C), the permeability of the liposomal membrane likely increased, which leads to higher release. The average of various statistical parameters was calculated for all of the tests, according to Peppas' model. The average R^2 and RMSE were 0.9587 and 0.0653, respectively. This indicated that model predictions were very close to experimental data. In addition, the release exponents values for all conditions under study were less than 0.5; therefore, it was concluded that the mechanism of release obeyed Fickian diffusion.

Rostamizadeh *et al.* [66] studied the kinetics of drug release from methotrexate (MTX) copolymeric conjugated

TABLE IV
SUMMARY OF STUDIES FOCUSED ON KINETIC MODELING OF RELEASE FROM US-TRIGGERED MICELLES AND LIPOSOMES.

Carrier type	Payload	Remarks on drug release	Ref.
Pluronic® P105 micelles	DOX	• The Keller–Miksis dynamic model predicted the release behavior of DOX from polymeric micelles.	[88]
Pluronic® P105 micelles	DOX	• The Parlitz modification of the Keller–Miksis model gave solutions similar to the Fourier transformed frequency spectra of the bubble oscillations. • Drug release from Pluronic micelles was observed at 70 kHz, but not at 500 kHz.	[89]
Nanoemulsions	perfluorocarbon	• The model verified the predictions of the heat, mass and momentum transport phenomena that occur during acoustic droplet vaporization.	[90]
Pluronic® P-105 and folate-targeted Pluronic® P105	DOX	• The optimal release estimate was obtained by probabilistically adding the estimates from the hypothesized KF estimates and was able to account for the uncertainty in the system	[91]
Liposomes	Calcein	• The ANN system was able to follow the set point by varying the US intensity within preset constraints. • The system simulated model showed a high average fit with variable input variations, indicating the robustness of the non-linear model.	[92]
Pluronic® P-105	DOX	• The MLE-optimized filters proved to outperform the other estimators in predicting micellar release using US.	[93]
Unstabilized Pluronic® P105	DOX	• The release and re-encapsulation profiles were fit using a 4-parameter model	[76]
Liposomes	Calcein	• The drug release pattern followed first-order kinetics and increased with exposure time to a maximal release.	[77]
Pluronic® P105 micelles	DOX	• The non-linear NN-MPC controller was effective in controlling the release of DOX from unstabilized micelles at different frequencies, power intensities and acoustic pulses.	[75]

micelles under different pH values by different kinetic models, including zero-order, first-order, Hill equation, Hixson–Crowell, Korsmeyer–Peppas, and Weibull. The release results showed no considerable initial burst MTX release from the micelles; furthermore, the percentage of MTX released from the micelles increased as the pH value decreased from 7.4 to 5.5. This pH sensitivity of drug release from the conjugate micelles was attributed to the cleavage of the ester bonds at different values and the swelling of the matrix in acidic environments due to the protonation of the polymer. The study concluded that, at pH 7.4, the MTX release data were adequately fit using the zero-order model ($R^2 = 0.8108$); while the kinetic release study at pH 5.5 confirmed that the MTX release data adequately fit the zero-order ($R^2 = 0.8410$), Higuchi ($R^2 = 0.8318$), Korsmeyer–Peppas ($R^2 = 0.8336$), and Weibull models ($R^2 = 0.8574$). Lu and Ten Hagen [67] studied the release kinetics of thermosensitive liposomes (TSLs). The author's fit their release data using several kinetic models commonly mentioned in literature (the nine kinetic models presented in section III of this review) and found that only the Korsmeyer-Peppas and Weibull models showed acceptable fitting results. They then proposed a new equation in which the Laplace pressure is the driving force that can describe the release from TSLs as small as 70 nm. The developed model showed desirable fitting across the entire release-temperature range, for both large and small-size liposomes.

US-triggered drug release from micelles and liposomes is another promising triggering modality with many advantages such as non-invasiveness, low cost, and easy accessibility. US offers spatiotemporal control of drug release and has shown good synergism when administered in conjunction with therapeutic agents. The drug release mechanism from US-triggered polymeric micelles was rigorously investigated by Husseini *et al.* [68]–[75]. In addition, Stevenson-Abouelnasr *et al.* [76] studied the release mechanisms and kinetics of DOX from Pluronic P105 micelles exposed to US. The proposed kinetic model was solved numerically for a sonication period of 60 s and compared to the experimental drug release data; values for the constants appearing in the model were determined using the best fit to the experimental data. The model was found to be an excellent fit to the experimental data, and a close agreement was achieved for each phase of the release.

Afadzi *et al.* [77] investigated the effects of US parameters on calcein release from dierucoyl-phosphatidylcholine (DEPC)-based liposomes at 2 frequencies, namely, 300 kHz and 1 MHz. The US-induced release experiments showed that the release was more efficient at 300 kHz than at 1 MHz, and that calcein release followed first-order kinetics and increased with exposure time. In another study, Wadi *et al.* [78] investigated the mathematical modeling of calcein release from albumin-, estrone-, and RGD-conjugated US-triggered liposomes. Five models were investigated, namely, zero-order, first-order, Higuchi, Korsmeyer-Peppas, and Gompertz models. The models were first studied to determine the best fit for the experimental data. Then, an adaptive variant of a Kalman filter (AKF) was designed to use the dynamics and measurements models, while adaptively estimating the noise covariance magnitudes. The best-fitting models were determined using the Mean Square Errors (MSE). Accordingly, the first-order and the Gompertz models were the best fit for the experimental data (both had low and comparable MSE). However, the first-order model, was selected due to its simple form which can be exploited in applying the AKF. With respect to filtering, the AKF approach, in comparison with the KF, exhibited a lower reduction in the level of error in estimating the drug release state (69%).

TABLE III and TABLE IV provide a summary of some relevant studies pertaining to the kinetic modeling of chemotherapeutic drug release from micelles and liposomes.

VI. Conclusion and Future Perspectives

Mathematical models have greatly enhanced our understanding of the mechanisms involved in drug release from drug delivery systems and have helped guide the design of these platforms. In this review, we explored the different drug release mechanisms from nanocarriers and summarized nine mathematical models frequently utilized to capture drug release kinetics. Many drug delivery systems can be modeled using one of these mathematical representations, including stimuli-triggered micelles and liposomes; however, no single model can aptly describe all the release data since the drug release generally depends on the size and composition of the carrier as well as the type of drugs and the loading techniques.

Several obstacles need to be addressed to ensure a more holistic and realistic modeling of drug delivery from nanocarriers. In order to close the gap between experiments and theory, we need accurate molecular, thermodynamic, and transport parameters. Another direction that requires further research is the *in vitro* conditions in which drug release kinetics are tested. In the development stage, the most widely used release medium is buffered saline, which does not reflect the complexity of blood, as serum proteins and lipids can greatly challenge the stability of nanocarriers. Consequently, it is often observed that drug release in serum-complemented cell culture medium or in blood occurs much faster than that predicted in buffered saline [1], [5], [15], [26]. Additionally, it is important to develop methods to examine drug release profiles in physiological environments where the assumption for sink conditions does not hold, i.e., when the target tissues contain a limited amount of fluid (e.g., lungs), and when the delivered drug has limited water solubility and low transepithelial permeability [1], [15]. The majority of the drugs currently used in drug delivery models are small molecular weight drugs. However, given the present-day interest in protein-based drugs and antigens, it is necessary to develop accurate models of protein delivery, which account for the conformational changes of proteins and the alterations in the protein structure during the synthesis of the nanocarrier and subsequent release [15].

Currently, the fitting of dissolution data can be performed using Microsoft Excel templates or professional statistical software packages such as MicroMath Scientist, GraphPad Prism, SigmaPlot, or SYSTAT. However, these programs require the user to define the equation manually and provide an initial value for each parameter. This may cause difficulty for new users and is not friendly to researchers who do not have advanced skills in computer programming [49]. Therefore, it is necessary to develop easy-to-use programs for fitting release data with more ready-to-use dissolution models. A number of programs have been developed, such as KinetDS, which can be used for the curve fitting of release kinetics (mechanistic and empirical). In the current version of this software, all models can be linearized. Therefore, the data can be fit using both linear regression and non-linear regression [79]. Another developed software is DDSolver, a versatile and freely available add-in program, which consists of a built-in model library containing forty dissolution models that can be used to facilitate the modeling of dissolution data using non-linear optimization methods. This program can also be used to simplify the task of assessing the similarity between dissolution profiles and the suitability of each model. Developing specialized programs for the analysis of kinetic release data is an essential tool that needs further attention because it helps speed up the calculation, reduce user errors, and provide a convenient way to report dissolution data quickly and easily [49], [80].

Conflicts of Interest

There are no conflicts to declare.

Abbreviations

ANOVA	Analysis of variance
Au NP	Gold nanoparticle
BBB	Blood-brain barrier
CNT	Carbon nanotube
DDS	Drug delivery system
DOX	Doxorubicin
DTX	Docetaxel
EDA	Exploratory data analysis
EPR effect	Enhanced permeability and retention effect
IMC	Indometacin
MANOVA	Multivariate analysis of variance
MEC	Minimum effective concentration
MTC	Minimum toxic concentration
MTX	Methotrexate
NP	Nanoparticle
PCL	Polycaprolactone
PLA	Polylactic acid
PLGA	Poly(lactic-co-glycolic acid)
QD	Quantum dot
US	Ultrasound

References

[1] J. H. Lee and Y. Yeo, "Controlled drug release from pharmaceutical nanocarriers," *Chem. Eng. Sci.*, vol. 125, pp. 75–84, Mar. 2015, doi: 10.1016/j.ces.2014.08.046.

[2] D. Peer, J. M. Karp, S. Hong, O. C. Farokhzad, R. Margalit, and R. Langer, "Nanocarriers as an emerging platform for cancer therapy," *Nature Nanotechnol.*, vol. 2, no. 12, pp. 751–760, Dec. 2007, doi: 10.1038/nnano.2007.387.

[3] F. U. Din *et al.*, "Effective use of nanocarriers as drug delivery systems for the treatment of selected tumors," *Int. J. Nanomed.*, vol. 12, pp. 7291–7309, Oct. 2017, doi: 10.2147/IJN.S146315.

[4] D. Ghosh, N. Upmanyu, T. Shukla, and T. P. Shrivastava, "Cell and organ drug targeting," in *Nanomaterials for Drug Delivery and Therapy*. Amsterdam, The Netherlands: Elsevier, 2019, pp. 1–31.

[5] M. L. Bruschi, "Mathematical models of drug release," in *Strategies to Modify the Drug Release From Pharmaceutical Systems*. Sawston, U.K.: Woodhead Publishing, 2015, pp. 63–86.

[6] A. Frère, B. Evrard, D. Mottet, and G. Piel, "Polymeric nanoparticles as siRNA drug delivery system for cancer therapy: The long road to therapeutic efficiency," in *Nanoarchitectonics for Smart Delivery and Drug Targeting*. Amsterdam, The Netherlands: Elsevier, 2016, pp. 503–540.

[7] A. Bose and T. W. Wong, "Oral colon cancer targeting by chitosan nanocomposites," in *Applications of Nanocomposite Materials in Drug Delivery*. Amsterdam, The Netherlands: Elsevier, 2018, pp. 409–429.

[8] A. Jain and S. K. Jain, "Advances in tumor targeted liposomes," *Current Mol. Med.*, vol. 18, no. 1, pp. 44–57, Jul. 2018, doi: 10.2174/1566524018666180416101522.

[9] M. Riaz *et al.*, "Surface functionalization and targeting strategies of liposomes in solid tumor therapy: A review," *Int. J. Mol. Sci.*, vol. 19, no. 1, p. 195, Jan. 2018, doi: 10.3390/ijms19010195.

[10] S. D. Steichen, M. Caldorera-Moore, and N. A. Peppas, "A review of current nanoparticle and targeting moieties for the delivery of cancer therapeutics," *Eur. J. Pharmaceutical Sci.*, vol. 48, no. 3, pp. 416–427, Feb. 2013, doi: 10.1016/j.ejps.2012.12.006.

[11] Y. Lee and D. H. Thompson, "Stimuli-responsive liposomes for drug delivery," *Wiley Interdiscipl. Rev., Nanomed. Nanobiotechnol.*, vol. 9, no. 5, p. e1450, Sep. 2017, doi: 10.1002/wnan.1450.

[12] N. M. Al Sawaftah and G. A. Husseini, "Ultrasound-mediated drug delivery in cancer therapy: A review," *J. Nanosci. Nanotechnol.*, vol. 20, no. 12, pp. 7211–7230, Dec. 2020, doi: 10.1166/jnn.2020.18877.

[13] A. Fick, "Ueber diffusion," *Ann. Phys.*, vol. 170, no. 1, pp. 59–86, Jan. 1855, doi: 10.1002/andp.18551700105.

[14] R. A. Siegel, *Fundamentals and Applications of Controlled Release Drug Delivery* (Advances in Delivery Science and Technology), J. Siepmann, R. A. Siegel, and M. J. Rathbone, Eds. New York, NY, USA: Springer, 2012, pp. 19–43, doi: 10.1007/978-1-4614-0881-9.

[15] N. A. Peppas and B. Narasimhan, "Mathematical models in drug delivery: How modeling has shaped the way we design new drug delivery systems," *J. Controlled Release*, vol. 190, pp. 75–81, Sep. 2014, doi: 10.1016/j.jconrel.2014.06.041.

[16] R. A. Peattie, R. J. Fisher, J. D. Bronzino, and D. R. Peterson, *Transport Phenomena in Biomedical Engineering: Principles and Practices*. Boca Raton, FL, USA: CRC Press, 2012.

[17] W. M. Saltzman, *Drug Delivery: Engineering Principles for Drug Therapy*. London, U.K.: Oxford Univ. Press, 2001.

[18] J. Crank, *The Mathematics of Diffusion*, 2nd ed. London, U.K.: Oxford Univ. Press, 1973.

[19] C. K. Sahoo, S. Ram, M. Rao, M. Sudhakar, and N. K. Sahoo, "Advances in osmotic drug delivery system," *J. Chem. Pharmaceutical Res.*, vol. 7, no. 7, pp. 252–273, 2015. [Online]. Available: https://www.jocpr.com

[20] L. Shu *et al.*, "Modified Kedem–Katchalsky equations for osmosis through nano-pore," *Desalination*, vol. 399, pp. 47–52, Dec. 2016, doi: 10.1016/j.desal.2016.08.011.

[21] T. Boissenot, A. Bordat, E. Fattal, and N. Tsapis, "Ultrasound-triggered drug delivery for cancer treatment using drug delivery systems: From theoretical considerations to practical applications," *J. Controlled Release*, vol. 241, pp. 144–163, Nov. 2016, doi: 10.1016/j.jconrel.2016.09.026.

[22] S. M. Janib, A. S. Moses, and J. A. MacKay, "Imaging and drug delivery using theranostic nanoparticles," *Adv. Drug Del. Rev.*, vol. 62, no. 11, pp. 1052–1063, Aug. 2010, doi: 10.1016/j.addr.2010.08.004.

[23] J. Wallyn, N. Anton, S. Akram, and T. F. Vandamme, "Biomedical imaging: Principles, technologies, clinical aspects, contrast agents, limitations and future trends in nanomedicines," *Pharmaceutical Res.*, vol. 36, no. 6, pp. 1–31, Jun. 2019, doi: 10.1007/s11095-019-2608-5.

[24] M. Sivasubramanian, Y. Hsia, and L.-W. Lo, "Nanoparticle-facilitated functional and molecular imaging for the early detection of cancer," *Frontiers Mol. Biosci.*, vol. 1, pp. 1–15, Oct. 2014, doi: 10.3389/fmolb.2014.00015.

[25] C. S. Brazel and N. A. Peppas, "Mechanisms of solute and drug transport in relaxing, swellable, hydrophilic glassy polymers," *Polymer*, vol. 40, no. 12, pp. 3383–3398, Jun. 1999, doi: 10.1016/S0032-3861(98)00546-1.

[26] G.-H. Son, B.-J. Lee, and C.-W. Cho, "Mechanisms of drug release from advanced drug formulations such as polymeric-based drug-delivery systems and lipid nanoparticles," *J. Pharmaceutical Invest.*, vol. 47, no. 4, pp. 287–296, Jul. 2017, doi: 10.1007/s40005-017-0320-1.

[27] D. M. Brahankar and S. B. Jaiswal, *Biopharmaceutics and Pharmacokinetics: A Treatise*. New Delhi, India: Vallabh Prakashan, 2009.

[28] S. Dash, P. N. Murthy, L. Nath, and P. Chowdhury, "Kinetic modeling on drug release from controlled drug delivery systems," *Acta Poloniae Pharmaceutica*, vol. 67, no. 3, pp. 23–217, 2010.

[29] Y. Shi, A. Wan, Y. Shi, Y. Zhang, and Y. Chen, "Experimental and mathematical studies on the drug release properties of aspirin loaded chitosan nanoparticles," *BioMed Res. Int.*, vol. 2014, pp. 1–8, Jan. 2014, doi: 10.1155/2014/613619.

[30] N. Shahrin, "Solubility and dissolution of drug product: A review," *Int. J. Pharmaceutical Life Sci.*, vol. 2, no. 1, pp. 33–39, 2013.

[31] N. M. Alsawaftah, "The use of transferrin and ultrasound in cancer treatment," M.S. thesis, Amer. Univ. Sharjah, Sharjah, United Arab Emirates, 2019.

[32] H. Baishya, "Application of mathematical models in drug release kinetics of carbidopa and levodopa ER tablets," *J. Developing Drugs*, vol. 6, no. 2, p. 171, 2017, doi: 10.4172/2329-6631.1000171.

[33] D. Shi, Ed., *Biomedical Devices and Their Applications*, 1st ed. New York, NY, USA: Springer-Verlag, 2004.

[34] N. Kamaly, B. Yameen, J. Wu, and O. C. Farokhzad, "Degradable controlled-release polymers and polymeric nanoparticles: Mechanisms of controlling drug release," *Chem. Rev.*, vol. 116, no. 4, pp. 2602–2663, 2016, doi: 10.1021/acs.chemrev.5b00346.

[35] H. B. Hopfenberg, "Controlled release from erodible slabs, cylinders, and spheres," in *Controlled Release Polymeric Formulations*, D. R. Paul and F. W. Harris, Eds. American Cancer Society, 1976, pp. 26–32, doi: 10.1021/bk-1976-0033.ch003.

[36] M. Riaz *et al.*, "Surface functionalization and targeting strategies of liposomes in solid tumor therapy: A review," *Int. J. Mol. Sci.*, vol. 19, no. 1, p. 195, Jan. 2018, doi: 10.3390/ijms19010195.

[37] J. Siepmann and F. Siepmann, "Mathematical modeling of drug delivery," *Int. J. Pharmaceutics*, vol. 364, no. 2, pp. 328–343, Dec. 2008, doi: 10.1016/j.ijpharm.2008.09.004.

[38] J. Siepmann and N. A. Peppas, "Higuchi equation: Derivation, applications, use and misuse," *Int. J. Pharmaceutics*, vol. 418, no. 1, pp. 6–12, Oct. 2011, doi: 10.1016/j.ijpharm.2011.03.051.

[39] D. Y. Arifin, L. Y. Lee, and C.-H. Wang, "Mathematical modeling and simulation of drug release from microspheres: Implications to drug delivery systems," *Adv. Drug Del. Rev.*, vol. 58, nos. 12–13, pp. 1274–1325, Nov. 2006, doi: 10.1016/j.addr.2006.09.007.

[40] A. Shahiwala and A. Misra, "Nasal delivery of levonorgestrel for contraception: An experimental study in rats," *Fertility Sterility*, vol. 81, no. 1, pp. 893–898, Mar. 2004, doi: 10.1016/j.fertnstert.2003.10.015.

[41] D. C. Hoaglin, F. Mosteller, and J. W. Tukey, *Understanding Robust and Exploratory Data Analysis*. Hoboken, NJ, USA: Wiley, 1983.

[42] A. Minke, "Conducting repeated measures analyses: Experimental design considerations," ERIC, USA, Tech. Rep., 1997.

[43] W. Guthrie, "NIST/SEMATECH e-handbook of statistical methods," NIST/SEMATECH, Gaithersburg, MD, USA, Tech. Rep., 2010. [Online]. Available: http://www.itl.nist.gov/div898/handbook/

[44] N. T. Longford, "Multivariate analysis of variance," in *International Encyclopedia of Education*. Amsterdam, The Netherlands: Elsevier, 2010, pp. 319–323.

[45] V. P. Shah, Y. Tsong, P. Sathe, and R. L. Williams, "Dissolution profile comparison using similarity factor, f2," *Dissolution Technol.*, vol. 6, no. 3, pp. 1–2, 1999, doi: 10.14227/DT060399P15.

[46] Lonza. (2010). *Cell Assays and Analysis*. Accessed: Jan. 30, 2019. [Online]. Available: https://bioscience.lonza.com/lonza_bs/CH/en/primary-hepatocytes-admetox-information-quote-request?utm_campaign=C-00003405

[47] R. E. Apfel and C. K. Holland, "Gauging the likelihood of cavitation from short-pulse, low-duty cycle diagnostic ultrasound," *Ultrasound Med. Biol.*, vol. 17, no. 2, pp. 179–185, Jan. 1991, doi: 10.1016/0301-5629(91)90125-G.

[48] S. E. Ahmed, N. Awad, V. Paul, H. G. Moussa, and G. A. Husseini, "Improving the efficacy of anticancer drugs via encapsulation and acoustic release," *Current Topics Med. Chem.*, vol. 18, no. 10, pp. 857–880, Aug. 2018, doi: 10.2174/1568026618666180608125344.

[49] A. Jain and S. K. Jain, "*In vitro* release kinetics model fitting of liposomes: An insight," *Chem. Phys. Lipids*, vol. 201, pp. 28–40, Dec. 2016, doi: 10.1016/j.chemphyslip.2016.10.005.

[50] S. Taurin, H. Nehoff, T. Van Aswegen, and K. Greish, "Tumor vasculature, EPR effect, and anticancer nanomedicine: Connecting the dots," in *Cancer Targeted Drug Delivery: An Elusive Dream*, Y. H. Bae, R. J. Mrsny, and K. Park, Eds. New York, NY, USA: Springer, 2013, pp. 207–239.

[51] K. Greish, "Enhanced permeability and retention effect for selective targeting of anticancer nanomedicine: Are we there yet?" *Drug Discovery Today, Technol.*, vol. 9, no. 2, pp. e161–e166, Jun. 2012, doi: 10.1016/j.ddtec.2011.11.010.

[52] N. S. Awad *et al.*, "Ultrasound-responsive nanocarriers in cancer treatment: A review," *ACS Pharmacol. Transl. Sci.*, vol. 4, no. 2, pp. 589–612, Apr. 2021, doi: 10.1021/acsptsci.0c00212.

[53] H. Xia, Y. Zhao, and R. Tong, "Ultrasound-mediated polymeric micelle drug delivery," in *Therapeutic Ultrasound* (Advances in Experimental Medicine and Biology), vol. 880. New York, NY, USA: Springer, Jan. 2016, pp. 365–384, doi: 10.1007/978-3-319-22536-4_20.

[54] Z. Ahmad, A. Shah, M. Siddiq, and H.-B. Kraatz, "Polymeric micelles as drug delivery vehicles," *RSC Adv.*, vol. 4, no. 33, pp. 17028–17038, 2014, doi: 10.1039/c3ra47370h.

[55] E. V. Batrakova, T. K. Bronich, J. A. Vetro, and A. V. Kabanov, "Polymer micelles as drug carriers," in *Nanoparticulates as Drug Carriers*, V. P. Torchlin, Ed. London, U.K.: Imperial College Press, 2006, pp. 57–93.

[56] L. Tao, J. W. Chan, and K. E. Uhrich, "Drug loading and release kinetics in polymeric micelles: Comparing dynamic versus unimolecular sugar-based micelles for controlled release," *J. Bioactive Compatible Polym.*, vol. 31, no. 3, pp. 227–241, May 2016, doi: 10.1177/0883911515609814.

[57] H. Shibata, K.-I. Izutsu, C. Yomota, H. Okuda, and Y. Goda, "Investigation of factors affecting *in vitro* doxorubicin release from PEGylated liposomal doxorubicin for the development of *in vitro* release testing conditions," *Drug Develop. Ind. Pharmacy*, vol. 41, no. 8, pp. 1376–1386, Aug. 2015, doi: 10.3109/03639045.2014.954582.

[58] D. C. Drummond, O. Meyer, K. Hong, D. B. Kirpotin, and D. Papahadjopoulos, "Optimizing liposomes for delivery of chemotherapeutic agents to solid tumors," *Pharmacol. Rev.*, vol. 51, no. 4, pp. 691–743, Dec-1999.

[59] L. H. Lindner and M. Hossann, "Factors affecting drug release from liposomes," *Current Opinion Drug Discovery Develop.*, vol. 13, no. 1, pp. 111–123, Jan. 2010.

[60] K. D. Fugit *et al.*, "Mechanistic model and analysis of doxorubicin release from liposomal formulations," *J. Controlled Release*, vol. 217, pp. 82–91, Nov. 2015, doi: 10.1016/j.jconrel.2015.08.024.

[61] H. Y. Yoon *et al.*, "Docetaxel-loaded RIPL peptide (IPLVVPLRRRRRRRRC)-conjugated liposomes: Drug release, cytotoxicity, and antitumor efficacy," *Int. J. Pharmaceutics*, vol. 523, no. 1, pp. 229–237, May 2017, doi: 10.1016/j.ijpharm.2017.03.045.

[62] X. Lu *et al.*, "PEG-conjugated triacontanol micelles as docetaxel delivery systems for enhanced anti-cancer efficacy," *Drug Del. Transl. Res.*, vol. 10, no. 1, pp. 122–135, Feb. 2020, doi: 10.1007/s13346-019-00667-6.

[63] T. L. S. Lapenda *et al.*, "Encapsulation of trans-dehydrocrotonin in liposomes: An enhancement of the antitumor activity," *J. Biomed. Nanotechnol.*, vol. 9, no. 3, pp. 499–510, Mar. 2013, doi: 10.1166/jbn.2013.1554.

[64] S. Maritim, P. Boulas, and Y. Lin, "Comprehensive analysis of liposome formulation parameters and their influence on encapsulation, stability and drug release in glibenclamide liposomes," *Int. J. Pharmaceutics*, vol. 592, Jan. 2021, Art. no. 120051, doi: 10.1016/j.ijpharm.2020.120051.

[65] F. Haghiralsadat *et al.*, "A comprehensive mathematical model of drug release kinetics from nano-liposomes, derived from optimization studies of cationic PEGylated liposomal doxorubicin formulations for drug-gene delivery," *Artif. Cells, Nanomed., Biotechnol.*, vol. 46, no. 1, pp. 169–177, Jan. 2018, doi: 10.1080/21691401.2017.1304403.

[66] K. Rostamizadeh, M. Manafi, H. Nosrati, H. K. Manjili, and H. Danafar, "Methotrexate-conjugated mPEG–PCL copolymers: A novel approach for dual triggered drug delivery," *New J. Chem.*, vol. 42, no. 8, pp. 5937–5945, Apr. 2018, doi: 10.1039/c7nj04864e.

[67] T. Lu and T. L. M. T. Hagen, "A novel kinetic model to describe the ultra-fast triggered release of thermosensitive liposomal drug delivery systems," *J. Controlled Release*, vol. 324, pp. 669–678, Aug. 2020, doi: 10.1016/j.jconrel.2020.05.047.

[68] G. A. Husseini, L. Kherbeck, W. G. Pitt, J. A. Hubbell, D. A. Christensen, and D. Velluto, "Kinetics of ultrasonic drug delivery from targeted micelles," *J. Nanosci. Nanotechnol.*, vol. 15, no. 3, pp. 2099–2104, Mar. 2015, doi: 10.1166/jnn.2015.9498.

[69] G. A. Husseini, D. Stevenson-Abouelnasr, W. G. Pitt, K. T. Assaleh, L. O. Farahat, and J. Fahadi, "Kinetics and thermodynamics of acoustic release of doxorubicin from non-stabilized polymeric micelles," *Colloids Surf. A, Physicochem. Eng. Aspects*, vol. 359, nos. 1–3, pp. 18–24, Apr. 2010, doi: 10.1016/j.colsurfa.2010.01.044.

[70] G. A. Husseini, N. M. Abdel-Jabbar, F. S. Mjalli, W. G. Pitt, and A. Al-Mousa, "Optimizing the use of ultrasound to deliver chemotherapeutic agents to cancer cells from polymeric micelles," *J. Franklin Inst.*, vol. 348, no. 7, pp. 1276–1284, Sep. 2011, doi: 10.1016/j.jfranklin.2010.02.004.

[71] G. A. Husseini, W. G. Pitt, J. B. Williams, and M. Javadi, "Investigating the release mechanism of calcein from eLiposomes at higher temperatures," *J. Colloid Sci. Biotechnol.*, vol. 3, no. 3, pp. 239–244, Sep. 2014, doi: 10.1166/jcsb.2014.1100.

[72] G. A. Husseini, N. Y. Rapoport, D. A. Christensen, J. D. Pruitt, and W. G. Pitt, "Kinetics of ultrasonic release of doxorubicin from pluronic P105 micelles," *Colloids Surf. B Biointerfaces*, vol. 24, nos. 3–4, pp. 253–264, 2002, doi: 10.1016/S0927-7765(01)00273-9.

[73] G. A. Husseini, N. M. Abdel-Jabbar, F. S. Mjalli, and W. G. Pitt, "Modeling and sensitivity analysis of acoustic release of doxorubicin from unstabilized pluronic P105 using an artificial neural network model," *Technol. Cancer Res. Treatment*, vol. 6, no. 1, pp. 49–56, 2007, doi: 10.1177/153303460700600107.

[74] G. A. Husseini *et al.*, "Kinetics of acoustic release of doxorubicin from stabilized and unstabilized micelles and the effect of temperature," *J. Franklin Inst.*, vol. 348, no. 1, pp. 125–133, Feb. 2011, doi: 10.1016/j.jfranklin.2009.02.007.

[75] G. A. Husseini, F. S. Mjalli, W. G. Pitt, and N. M. Abdel-Jabbar, "Using artificial neural networks and model predictive control to optimize acoustically assisted doxorubicin release from polymeric micelles," *Technol. Cancer Res. Treat.*, vol. 8, no. 6, pp. 479–488, 2009, doi: 10.1177/153303460900800609.

[76] D. Stevenson-Abouelnasr, G. A. Husseini, and W. G. Pitt, "Further investigation of the mechanism of doxorubicin release from P105 micelles using kinetic models," *Colloids Surf. B, Biointerfaces*, vol. 55, no. 1, pp. 59–66, Mar. 2007, doi: 10.1016/j.colsurfb.2006.11.006.

[77] M. Afadzi *et al.*, "Effect of ultrasound parameters on the release of liposomal calcein," *Ultrasound Med. Biol.*, vol. 38, no. 3, pp. 476–486, Mar. 2012, doi: 10.1016/j.ultrasmedbio.2011.11.017.

[78] A. Wadi, M. Abdel-Hafez, G. A. Husseini, and V. Paul, "Multi-model investigation and adaptive estimation of the acoustic release of a model drug from liposomes," *IEEE Trans. Nanobiosci.*, vol. 19, no. 1, pp. 68–77, Jan. 2020, doi: 10.1109/TNB.2019.2950344.

[79] A. Mendyk, R. Jachowicz, K. Fijorek, P. Dorożyński, P. Kulinowski, and S. Polak, "KinetDS: An open source software for dissolution test data analysis," *Dissolution Technol.*, vol. 19, no. 1, pp. 6–11, 2012, doi: 10.14227/DT190112P6.

[80] Y. Zhang *et al.*, "DDSolver: An add-in program for modeling and comparison of drug dissolution profiles," *AAPS J.*, vol. 12, no. 3, pp. 263–271, Sep. 2010, doi: 10.1208/s12248-010-9185-1.

[81] S. Jain, S. R. Patil, N. K. Swarnakar, and A. K. Agrawal, "Oral delivery of doxorubicin using novel polyelectrolyte-stabilized liposomes (Layersomes)," *Mol. Pharmaceutics*, vol. 9, no. 9, pp. 2626–2635, Sep. 2012, doi: 10.1021/mp300202c.

[82] T. Wang, L. Gao, and D. Quan, "Multivesicular liposome (MVL) sustained delivery of a novel synthetic cationic GnRH antagonist for prostate cancer treatment," *J. Pharmacy Pharmacol.*, vol. 63, no. 7, pp. 904–910, Jun. 2011, doi: 10.1111/j.2042-7158.2011.01295.x.

[83] W. Hao, T. Xia, Y. Shang, S. Xu, and H. Liu, "Characterization and release kinetics of liposomes inserted by pH-responsive bola-polymer," *Colloid Polym. Sci.*, vol. 294, no. 7, pp. 1107–1116, Jul. 2016, doi: 10.1007/s00396-016-3871-1.

[84] K. Chakravarty and D. C. Dalal, "Mathematical modelling of liposomal drug release to tumour," *Math. Biosci.*, vol. 306, pp. 82–96, Dec. 2018, doi: 10.1016/j.mbs.2018.10.012.

[85] J. Chen, A. Ding, Y. Zhou, P. Chen, Y. Xu, and W. Nie, "Indometacin-loaded micelles based on star-shaped PLLA-TPGS copolymers: Effect of arm numbers on drug delivery," *Colloid Polym. Sci.*, vol. 297, no. 10, pp. 1321–1330, Oct. 2019, doi: 10.1007/s00396-019-04542-1.

[86] M. T. Haseeb, N. U. Khaliq, S. H. Yuk, M. A. Hussain, and S. Bashir, "Linseed polysaccharides based nanoparticles for controlled delivery of docetaxel: Design, *in vitro* drug release and cellular uptake," *J. Drug Del. Sci. Technol.*, vol. 49, pp. 143–151, Feb. 2019, doi: 10.1016/j.jddst.2018.11.009.

[87] Z. Karami, S. Sadighian, K. Rostamizadeh, M. Parsa, and S. Rezaee, "Naproxen conjugated mPEG–PCL micelles for dual triggered drug delivery," *Mater. Sci. Eng., C*, vol. 61, pp. 665–673, Apr. 2016, doi: 10.1016/j.msec.2015.12.067.

[88] M. A. D. de la Rosa, G. A. Husseini, and W. G. Pitt, "Mathematical modeling of microbubble cavitation at 70 kHz and the importance of the subharmonic in drug delivery from micelles," *Ultrasonics*, vol. 53, no. 1, pp. 97–110, Jan. 2013, doi: 10.1016/j.ultras.2012.04.004.

[89] M. A. D. de la Rosa, G. A. Husseini, and W. G. Pitt, "Comparing microbubble cavitation at 500 kHz and 70 kHz related to micellar drug delivery using ultrasound," *Ultrasonics*, vol. 53, no. 2, pp. 377–386, Feb. 2013, doi: 10.1016/j.ultras.2012.07.004.

[90] W. G. Pitt, R. N. Singh, K. X. Perez, G. A. Husseini, and D. R. Jack, "Phase transitions of perfluorocarbon nanoemulsion induced with ultrasound: A mathematical model," *Ultrason. Sonochem.*, vol. 21, no. 2, pp. 879–891, Mar. 2014, doi: 10.1016/j.ultsonch.2013.08.005.

[91] M. Abdel-Hafez and G. A. Husseini, "Predicting the release of chemotherapeutics from the core of polymeric micelles using ultrasound," *IEEE Trans. Nanobiosci.*, vol. 14, no. 4, pp. 378–384, Jun. 2015, doi: 10.1109/TNB.2015.2399100.

[92] H. G. Moussa, G. A. Husseini, N. Abel-Jabbar, and S. E. Ahmad, "Use of model predictive control and artificial neural networks to optimize the ultrasonic release of a model drug from liposomes," *IEEE Trans. Nanobiosci.*, vol. 16, no. 3, pp. 149–156, Apr. 2017, doi: 10.1109/TNB.2017.2661322.

[93] A. Wadi, M. Abdel-Hafez, and G. A. Husseini, "Identification of the uncertainty structure to estimate the acoustic release of chemotherapeutics from polymeric micelles," *IEEE Trans. Nanobiosci.*, vol. 16, no. 7, pp. 609–617, Oct. 2017, doi: 10.1109/TNB.2017.2736021.